



1

# 1 LACK OF MARINE ENTRY INTO MARMARA AND BLACK SEA-LAKES INDICATE 2 LOW RELATIVE SEA LEVEL DURING MIS 3 IN THE NORTHEASTERN 3 MEDITERRANEAN 4

5  
 6 Anastasia G. Yanchilina<sup>1</sup>, Celine Grall<sup>2</sup>, William B.F. Ryan<sup>2</sup>, Jerry F. McManus<sup>2</sup>, Candace  
 7 O. Major<sup>3</sup>

8 <sup>1</sup>Department of Earth and Planetary Sciences, Weizmann Institute of Science, Rehovot, Israel  
 9 7610001.

10 <sup>2</sup>Lamont-Doherty Earth Observatory, Columbia University, 61 Route 9W, Palisades, New  
 11 York 10964.

12 <sup>3</sup>National Science Foundation, 2415 Eisenhower Ave., Alexandria, Virginia 22314  
 13

14 **Correspondence:** Anastasia Yanchilina (anastasia.yanchilina@weizmann.ac.il)  
 15

## 16 Abstract

17  
 18 The Marine Isotope Stage 3 (MIS 3) is considered a period of persistent and rapid climate and sea level  
 19 variabilities during which eustatic sea level is observed to have varied by tens of meters. Constraints on local sea  
 20 level during this time are critical for further estimates of these variabilities. We here present constraints on relative  
 21 sea level in the Marmara and Black Sea regions in the northeastern Mediterranean, inferred from reconstructions  
 22 of the history of the connections and disconnections (partial or total) of these seas together with the global ocean.  
 23 We use a set of independent data from seismic imaging and core-analyses to infer that the Marmara and Black  
 24 Seas remained connected persistent freshwater lakes that outflowed to the global ocean during the majority of  
 25 MIS 3. Marine water intrusion during the early MIS-3 stage may have occurred into the Marmara Sea-Lake but  
 26 not the Black Sea-Lake. This suggests that the relative sea level was near the paleo-elevation of the Bosphorus sill  
 27 and possibly slightly above the Dardanelles paleo-elevation, ~80 mbsl. The Eustatic sea level may have been  
 28 even lower, considering the isostatic effects of the Eurasian ice sheet would have locally uplifted the topography  
 29 of the northeastern Mediterranean.  
 30

## 31 1. Introduction

32 Marine isotope stage 3 (MIS 3) is identified as the period between 60 and 25 kyr B.P.,  
 33 when regional and global climate fluctuated over a broad range of temperatures on millennial  
 34 time scales (Dansgaard et al. 1993, Members 2006). One particularly noteworthy and  
 35 intriguing aspect of MIS 3 is its characteristic sequence of abrupt climate fluctuations including  
 36 the iconic Dansgaard-Oeschger (D-O) bi-polar oscillations and Heinrich event iceberg  
 37 discharges with corresponding fluctuations in global sea level on the order of ~20-40 m (Siddall  
 38 et al. 2008). The eustatic sea level (ESL) during this period remains uncertain, with sea level  
 39 elevations that range as low as 87 meters below today's sea level (mbsl) to as high as 25 mbsl  
 40 (Siddall et al. 2008). The lack of existence of a rigorous constraint on ESL has implications



41 for understanding factors that control ice-sheet growth and collapse. Ice volume variations are  
42 additionally an important input into glacial isostatic adjustment (GIA) models (Pico et al.  
43 2016), that are in turn used to understand changes in the distribution of ice volume on the planet  
44 and its effect on local sea level. It should be noted that ESL is different from Relative Sea Level  
45 (RSL) as the RSL represents the elevation of the sea relative to the moving solid earth. The  
46 earth is moving notably because of isostatic adjustment of the earth's surface to the changes in  
47 the distribution of ice and water and the corresponding changes of the gravitational potential  
48 of the earth-ocean system (Lambeck et al. 2002b). Also, the RSL can be obtained from  
49 geological archives and ESL may be derived from these archives when the earth solid surface  
50 motions are properly considered.

51 Several methodologies have been employed to deduce the height of past ESL: 1) ice  
52 volume changes using oxygen isotope measurements of planktonic and benthic foraminifera  
53 (Bintanja et al. 2005, Shakun et al. 2015) (Fig. 1a and b), 2) elevated coral terraces (Cutler et  
54 al. 2003) (Fig. 1c), and 4) changes between brackish and fresh conditions in marginal basins  
55 (Van Daele et al. 2011, Pico et al. 2016, Pico et al. 2017). Reconstructing ESL from the benthic  
56 foraminiferal LR04  $\delta^{18}\text{O}$  record using an inverse ice-sheet climate model gives sea level  
57 estimates below 80 mbsl (Fig. 1a) (Bintanja et al. 2005). Isolating the ice volume from a  
58 compilation of planktonic foraminiferal  $\delta^{18}\text{O}$  records gives a global sea level that decreases  
59 from ~60 mbsl to 80 mbsl over the course of MIS 3 (Fig. 1b) (Shakun et al. 2015). U/Th dated  
60 coral terraces used as a relative sea level proxy (Lambeck et al. 2002b), suggest after  
61 considering a GIA correction, that the ESL was below 60 mbsl (Fig. 1c) (Yokoyama et al.  
62 2001, Peltier et al. 2006). More recent studies suggest shallower estimates of ESL during MIS  
63 3. Sediment cores taken from the Yellow River Delta that similarly record fluctuations  
64 between fresh and marine environments have been used to assert that ESL reached a peak of  
65 38 mbsl during an interval between 50 and 37 kyr (Pico et al. 2016). Similarly, records from  
66 the Albermarle Embayment on the U.S. Mid-Atlantic coast show a ESL peak level of 40 mbsl  
67 during MIS 3 (Pico et al. 2017). Geological archives provide RSL indices. RSL indices are  
68 critical to constrain the local ESL and Global Mean Sea Level models.

69 In this paper, we provide highstand thresholds on RSL in the Black Sea and Marmara  
70 Sea system to infer information about ESL during MIS 3 using a GIA model and provide  
71 valuable geological constraints on regional RSL reconstructions. In the modern configuration,  
72 Black Sea and Marmara Sea are connected to the global ocean via shallow Bosphorus and  
73 Dardanelles Straits to form an interconnected lake-ocean system (Çagatay 2003). During



74 glacial periods, this configuration can change if the RSL falls below the straits, cutting off  
 75 marine water entry. Here we use observations from geochemical records and seismic images  
 76 to reconstruct water connection and disconnection histories between the Black Sea, Marmara  
 77 Sea, and the global ocean. We show that the two lakes were freshwater, connected, and  
 78 outflowing excess freshwater to the East Mediterranean for a large fraction of MIS 3, with the  
 79 exception of a possible transient marine entry from 55 kyr B.P. to 44 kyr B.P. We then provide  
 80 different independent estimates on paleo-lake elevations and sill elevations to provide a  
 81 database of RSL estimates and discuss the possible implication on the local ESL. In this paper,  
 82 we will refer to the Sea of Marmara and the Black Sea as Marmara Sea-Lake and Black Sea-  
 83 Lake, taking into account their prior freshwater state.

84

## 85 **2. Inferred paleo-salinity in the Marmara Sea-Lake and Black Sea-Lake during MIS 3** 86 **from previous studies**

87 Previous studies have documented the  $\text{CaCO}_3$  accumulation in the Marmara Sea  
 88 (Çağatay et al. 2015) and Ca (%) accumulation in the Black Sea (Nowaczyk et al. 2012),  
 89 porewater  $\text{Cl}^-$  in the Marmara Sea (Aloisi et al. 2015) and Black Sea (Soulet et al. 2010), and  
 90 last,  $\delta^{18}\text{O}$  composition of the Black Sea mollusk record (Major et al. 2006, Yanchilina et al.  
 91 2017) and Marmara Sea mollusk record (Vidal et al. 2010).

92  $\text{CaCO}_3$ , although a proxy that cannot be used as a direct measurement of paleosalinity,  
 93 it can be used to interpret the connectivity between water bodies.  $\text{CaCO}_3$  in lakes reflects the  
 94 integration between sedimentation rate and  $\text{CO}_2$ -assimilation and pH-changes induced by  
 95 phytoplankton blooms. Higher  $\text{CaCO}_3$  becomes deposited during warmer periods when there  
 96 are more phytoplankton blooms relative to colder periods. Specific to our case, the Sea of  
 97 Marmara is small in volume relative to the volume of the Black Sea and also, does not have a  
 98 significant amount of independent river inflow. Hence, the temporal synchronicity of  $\text{CaCO}_3$   
 99 variability between both basins is inferred to reflect connectivity of the two lakes and to  
 100 indicate outflows of the Black Sea-Lake into the Marmara Sea-Lake. Although fresh, both  
 101 lakes are likely to have been somewhat alkaline in order to account for episodes of organic and  
 102 inorganic carbonate accumulation at times of rapid warming during each of the  
 103 Dansgaard/Oeschger events (Çağatay et al. 2015).

104 Porewater  $\text{Cl}^-$  measurements were  $\sim 50$  mmol/L in the Black Sea-Lake and 200-500  
 105 mmol/L in the Marmara Sea-Lake during MIS 3 before their connection to the global ocean at  
 106 9.3 kyr B.P. (Yanchilina et al. 2017) and 14 kyr B.P. (Aloisi et al. 2015), respectively.



107 Application of an advection/diffusion model allows to qualitatively deconstruct paleosalinity.  
 108 The modern values for the Sea of Marmara and the Black Sea are 620 mmol/L and 350 mmol/L  
 109 with the former corresponding to a salinity value of ~39 ppt (Soulet et al. 2010, Aloisi et al.  
 110 2015). Freshwater bodies typically have low porewater  $\text{Cl}^-$  composition (i.e.,  $< \sim 50$  mmol/L).  
 111 A decrease of porewater  $\text{Cl}^-$  towards these values would indicate that these bodies of water  
 112 were fresher in the past. After taking into account advection and diffusion, porewater  $\text{Cl}^-$  values  
 113 indicate both of the seas were fresh during MIS 3 and possibly also the late part of MIS 4  
 114 (Soulet et al. 2010, Aloisi et al. 2015).

115 The  $\delta^{18}\text{O}$  composition of the mollusks from the Black Sea is measured to be  $-6 \pm 1$  ‰  
 116 (Major et al. 2006, Yanchilina et al. 2017) and the  $\delta^{18}\text{O}$  composition of the Sofular Cave  
 117 stalagmites is measured to be  $-12 \pm 1$  ‰ during the MIS 3 (Fleitmann et al. 2009, Badertscher  
 118 et al. 2011). The resolution of the U/Th ages for the Sofular Cave stalagmites for MIS 3 is, on  
 119 average, 24 years (Fleitmann et al. 2009).  $\delta^{18}\text{O}$  of  $-6$  ‰ measured in the Black Sea mollusks  
 120 is the value that reflects the  $\delta^{18}\text{O}$  composition of the mollusks during the last glacial period,  
 121 MIS 2, when the Black Sea was shown to be a freshwater lake. The  $\delta^{18}\text{O}$  of  $-12$  ‰ of the  
 122 Sofular Cave stalagmites is shown to reflect the evaporation of Black Sea water with a constant  
 123 offset of  $-6$  ‰, the difference argued to account for fractionation of water as a consequence of  
 124 distillation effects (Fleitmann et al. 2009, Badertscher et al. 2011). Given the observation that  
 125 the  $\delta^{18}\text{O}$  of the Sofular Cave stalagmites remains at  $-12$  ‰ all throughout MIS 3 indicates the  
 126 Black Sea was also fresh for the entirety of this period. Furthermore, freshwater mollusk  
 127 *Dreissena rostriformis*, and dinoflagellates *S. cruciformis* and *P. psilata* persistently dominate  
 128 the MIS 3 faunal composition in the Black Sea-Lake (Rochon et al. 2002, Yanchilina et al.  
 129 2017).

130 We will further evaluate these observations and prior interpretations from comparison  
 131 of variations in  $^{87}\text{Sr}/^{86}\text{Sr}$  measured in ostracod and mollusk shells from both Black Sea and  
 132 Marmara Sea basins. Contrary to the  $\delta^{18}\text{O}$  composition of water, a variable that incorporates  
 133 changes in the hydrological cycle of lake systems,  $^{87}\text{Sr}/^{86}\text{Sr}$  of water responds exclusively to  
 134 changes in source of water and can differentiate between changes in input from the different  
 135 sources.  $^{87}\text{Sr}/^{86}\text{Sr}$  is especially relevant to measure when making an attempt to identify inputs  
 136 of saline water into lake systems. Because of the low concentration of freshwater Sr from rivers,  
 137 even a small input of marine water, rich in Sr, will make an observable change in the  $^{87}\text{Sr}/^{86}\text{Sr}$   
 138 composition of freshwater bodies of water.  $^{87}\text{Sr}/^{86}\text{Sr}$  is a very sensitive proxy used previously  
 139 to reconstruct the deglacial entry of marine water into the Black Sea-Lake during the Holocene



(Major et al. 2006, Yanchilina et al. 2017). The modern  $^{87}\text{Sr}/^{86}\text{Sr}$  composition of river water inflowing into the Black Sea is  $\sim 0.7088$  (Palmer et al. 1989) whereas the  $^{87}\text{Sr}/^{86}\text{Sr}$  composition of the ocean water is 0.709155 (Henderson et al. 1994).

### 3. Materials and Methods

#### 3.1 Geochemistry

We measured  $^{87}\text{Sr}/^{86}\text{Sr}$  of ostracodes and mollusks from the Marmara Sea sediments and compared these measurements with the published values from the Black Sea (Major et al. 2006, Yanchilina et al. 2017). The sediments were taken from cores ITU-C1 at 73 mbsl, MD01-2426 at 250 mbsl, ITU-C10 at 364 mbsl, and MD01-2430 at 580 mbsl (Fig. 2). MD01-2426 and MD01-2430 were retrieved in 2001 during the MD123/MARMACORE cruise (R/V Marion Dufresne). MD01-2426 was collected from north of the Imrali ridge and MD01-2430 was collected on the Western High between the Central and the Tekirdag deep basins (Grall et al. 2013). ITU-C1 and -C10 were retrieved in 2002 with R/V MTA Sismik 1 in and around the Sarkoy Canyon in the Western Marmara Sea. The  $^{87}\text{Sr}/^{86}\text{Sr}$  records for the Sea of Marmara were measured at Lamont-Doherty Earth Observatory, Columbia University. Sr was initially leached to retrieve the Sr fraction (Bailey et al. 2000) which was then loaded upon tungsten filaments with TaCl<sub>5</sub> (Birck 1986).  $^{87}\text{Sr}/^{86}\text{Sr}$  ratios were measured using a dynamic multi-collector on a VG thermal ionization mass spectrometer and normalized to  $^{86}\text{Sr}/^{88}\text{Sr} = 0.1194$  to correct for mass fractionation. Beam size was tuned to be close to  $5.0 \times 10^{-11}$  for  $^{88}\text{Sr}$ .  $^{87}\text{Sr}/^{86}\text{Sr}$  measurements were monitored to account for instrumental drift through periodically running NBS987 which gave  $^{87}\text{Sr}/^{86}\text{Sr} = 0.710288 (\pm 0.000015)$  with a  $2\sigma$  external reproducibility,  $n = 16$ . The original age model was constructed from  $^{14}\text{C}$  measurements and calibrated to calendar age with a zero reservoir correction. Although the original  $^{14}\text{C}$  measurements have been misplaced, we compose our own age model from  $^{14}\text{C}$  measurements made from pieces of mollusks from MD01-2430 (Vidal et al. 2010) which we correct for reservoir after tuning its  $\delta^{18}\text{O}$  record to that of the Black Sea and Sofular Cave  $\delta^{18}\text{O}$  records. This procedure follows from the observation that the  $\delta^{18}\text{O}$  of the Sofular Cave  $\delta^{18}\text{O}$  record reflects the  $\delta^{18}\text{O}$  composition of Black Sea surface water (Fleitmann et al. 2009, Badertscher et al. 2011) which, before the connection of the Marmara Sea-Lake with the Mediterranean Sea reflected predominantly the  $\delta^{18}\text{O}$  composition of the Black Sea-Lake that flowed through the Bosphorus Strait into the Sea of Marmara. The results are presented in Supplementary Materials 1 and illustrated in Fig. 3 a.



6

173

### 174 3.2 Chirp profiles

175 We present a chirp record of a perched pond/lake, lake Gemlik (Figs. 2, 4), from Sea  
 176 of Marmara in order to diagnose whether any marine entry occurred during MIS 3. The chirp  
 177 profile was acquired during Sensing the Ocean with Marine Radars (SoMAR) cruise on the  
 178 R/V *K. Piri Reis* in 2013 with SyQwest-Bathy 2010 chirp profiler and operating frequency of  
 179 3.5 KHz. This perched lake is observed on the southern shelf of the Marmara Sea (Fig. 2). It  
 180 is separated from the deeper sections of the Marmara Sea by the Imrali ridge with a depth of  
 181 50 mbsl. Lake Bandirma is also indicated (Fig. 2) observed to lie to the east of Lake Gimlik  
 182 but a chirp profile for was not acquired.

183

## 184 4. Results

185

### 186 4.1 Paleosalinity and paleo-connectivity of Marmara and Black Sea during MIS 3

187  $^{87}\text{Sr}/^{86}\text{Sr}$  measurements of the Marmara Sea mollusks at the beginning of MIS 2 vary  
 188 around 0.7088 (Figure 3a), a value that is similar to the  $^{87}\text{Sr}/^{86}\text{Sr}$  composition of the Black Sea  
 189 during this period and also to the average  $^{87}\text{Sr}/^{86}\text{Sr}$  composition of river water flowing into the  
 190 Black Sea of 0.7088 (Palmer and Edmond 1989).  $^{87}\text{Sr}/^{86}\text{Sr}$  composition of Black Sea mollusks  
 191 also has a strictly lacustrine composition of  $0.70880 \pm 5 \times 10^{-5}$  at the end of MIS 3 (Fig. 3a). The  
 192  $^{87}\text{Sr}/^{86}\text{Sr}$  of freshwater mollusks from the Marmara Sea-Lake follows closely that of the Black  
 193 Sea record through the deglaciation and is also lacustrine at the beginning of MIS 2. For the  
 194 two lakes to share the identical  $^{87}\text{Sr}/^{86}\text{Sr}$  composition similar to the composition of river inflow  
 195 into the Black Sea, the Black Sea must have been fresh and outflowing to the Sea of Marmara.  
 196 The Sea of Marmara must have subsequently outflowed to the Mediterranean Sea, as it's a  
 197 much smaller volume relative to the Black Sea. We present supporting data to contest that the  
 198 two lakes were freshwater, connected, and outflowing excess freshwater to the East  
 199 Mediterranean for a large fraction of MIS 3.

200 Comparing together sediment Ca and  $\text{CaCO}_3$  (Nowaczyk et al. 2012, Çağatay et al.  
 201 2015) (Fig. 3b) with the porewater  $\text{Cl}^-$  (Soulet et al. 2010, Aloisi et al. 2015) (Fig. 3c) from the  
 202 Black and Marmara Seas and Sofular Cave  $\delta^{18}\text{O}$  of the stalagmites (Fleitmann et al. 2009,  
 203 Badertscher et al. 2011) (Fig. 3d) support this interpretation. The Ca and  $\text{CaCO}_3$  of the Black  
 204 Sea-Lake and Marmara Sea-Lake are identical for all of MIS 3 with the exception of the period  
 205 from 55 to 44 kyr B.P., in which either the Black Sea-Lake suspended outflow to the Marmara  
 206 Sea-Lake and/or there was a potential marine entry into the Marmara Sea-Lake but not the



7

207 Black Sea-Lake. The latter is less likely to have occurred as every marine entry recorded into  
 208 both the Marmara and Black Sea-Lakes is followed by a formation of a sapropel, evidence of  
 209 which here is not observed. We still consider this possibility in case the transient marine entry  
 210 was minor and perhaps was just a small inflow.

211 Porewater Cl<sup>-</sup> in Marmara Sea-Lake sediments differs from that of the Black Sea-Lake  
 212 sediments as a result of the earlier connection of the Marmara Sea with the global ocean and  
 213 higher post-connection salinity, leading to an earlier diffusion of marine water into the  
 214 previously lacustrine sediments. If there had been any marine inflow into either sea during  
 215 MIS 3, there would be observable remnant diffusion trends. In fact, Cl<sup>-</sup> decreases back through  
 216 time and into MIS 4 to 100 mmol/L, suggesting the Marmara Sea-Lake was also fresh during  
 217 this period and the freshening had to have happened even earlier. There is only one point  
 218 during which the Cl<sup>-</sup> is observed to increase, 50 kyr B.P., and we discuss this in this paper,  
 219 with the light of supplemental Sr analyses. Pore-water chloride,  $\delta^{18}\text{O}$  and  $^{87}\text{Sr}/^{86}\text{Sr}$  of mollusks  
 220 and ostracods do not indicate any significant rises in salinity in the Marmara and Black Sea-  
 221 Lakes.

222  $\delta^{18}\text{O}$  composition of the Sofular Cave stalagmites, porewater Cl<sup>-</sup> and sediment CaCO<sub>3</sub>  
 223 results support this interpretation. The  $\delta^{18}\text{O}$  of Black Sea-Lake and Marmara Sea-Lake  
 224 carbonate reflects the composite of hydrological balance in the basin through integration of  
 225 inputs in the form of river and rain water and outputs in the form of evaporative processes  
 226 (Major et al. 2006). A lower  $\delta^{18}\text{O}$  value is considered to be fresh and in a positive hydrological  
 227 framework whereas a higher  $\delta^{18}\text{O}$  value is considered to reflect either entrance of marine water  
 228 and/or a drier climate, preferentially removing the lighter oxygen isotope (i.e.,  $^{16}\text{O}$ ) from the  
 229 water (Deuser 1972). We use the  $\delta^{18}\text{O}$  composition of the dated Sofular Cave stalagmites with  
 230 a temporal resolution of  $\delta^{18}\text{O}$  measurements of ~24 years to infer the paleosalinity further back  
 231 in time, a measurement previously shown to reflect the composition of the Black Sea water  
 232 vapor (Badertscher et al. 2011). The most recent entry of marine water resulted in a rapid  
 233 increase in salinity to modern values in both the Black Sea-Lake (Major et al. 2006; Yanchilina  
 234 et al. 2017) and in the Marmara Sea-Lake (Sperling et al. 2003). This is not observed on the  
 235  $\delta^{18}\text{O}$  records, suggesting both basins remain fresh.

236

#### 237 4.2 MIS 3 Relative Sea Level Index in Marmara Sea-Lake and Black Sea-Lake.

238 Wave-cut cliffs and their corresponding terraces are observed everywhere in the  
 239 subsurface of the outermost Marmara Sea continental shelf at elevations close to the modern





Dardanelles bedrock sill at ~65 mbsl (Gokasan et al. 2008) (Supplementary Material 2-6, Table 1). At the distal edge of each terrace, one observes inclined clinoforms (Çağatay et al. 2009) indicative of subaqueous prodelta foresets that are truncated by an erosion surface (Vardar et al. 2014). Where sampled, the youngest foresets of these clinoforms are of early MIS-2 age (Yaltirak et al. 2002, Ergin et al. 2007, Çağatay et al. 2009, Karakilcik et al. 2014, Vardar et al. 2014). The mollusk assemblage, composed of exclusively freshwater species (i.e., *Dreissena r.*) in core MD04-2745 that sampled the entire succession of incline strata, indicates there was no observable entry of marine water during MIS 4, 3, and 2. Older MIS 5 deposits outcrop at elevations up to 7 m above today's sea level on the edge of the Dardanelles Strait (Supplementary Material 6, Table 1) (Yaltirak et al. 2002).

**Table 1**

Figure name	Source	Key observations
SU 2	Gökaşan et al. (2010)	MIS 2-3-4 foresets in the Marmara Sea-Lake, seaward of Prince Islands, below 80 mbsl
SU 3	Karakilcik et al. (2014)	MIS 2-3-4 foresets in the Marmara Sea-Lake, Çekmeke shelf break, lower than 90 mbsl
SU 4	Ergin et al. (2007)	MIS 2-3-4 foresets, northwest margin of Marmara Sea, lower than 75 mbsl. The youngest foreset is <sup>14</sup> C dated to MIS 2.
SU 5	Smith et al. (1995)	MIS 2-3-4 foresets, west of Imrali Island in the Marmara Sea, lower than 70 mbsl.
SU 6	Gökaşan et al. (2010)	Paleo-elevation of the Dardanelles strait is inferred to be 85 mbsl.

In the southern shelf of the Marmara Sea, both the Gemlik and Bandirma lakes are interpreted to have been separated from the large main Marmara Sea-Lake by the Imrali ridge during MIS 2, 3, and 4 (Vardar et al. 2014) (Fig. 4). Chirp records show no evidence at all of MIS 3 and 2 sediments on the shelves except in these perched ponds. The paleo-shorelines of the Bandirma and Gemlik suspended lakes are observed at ~50 mbsl and ~60 mbsl, respectively (Vardar et al. 2014). Thin transparent layers of Holocene age are observed on the Imrali Ridge, lying along an erosional unconformity (C-a) which has been interpreted as the last marine lacustrine to marine transition. A second deeper unconformity is observed below, on the intervening shelf region as well beneath the floor of the ponded lakes (Fig. 4). The age of the deeper unconformity is unconstrained, due to the lack of recovered sediment. It has been proposed that this unconformity may be 23 kyr or 30 kyr (Hiscott et al. 2002, Vardar et al. 2014). This observation, however, is not compatible with the stratigraphic history of the





deposits. It is shown that the MIS-2 period corresponds to a large transgressive period following the MIS-3 low stand (Çağatay et al. 2009). This suggests that the basal surface of the sediment deposited during MIS-2 should be conformable with sediment below. It is likely that this erosional surface is a consequence of the brief drying event related to the beginning of the Bolling/Allerød, immediately before entry of marine water into the Marmara Sea-Lake (McHugh et al. 2008). The bumps and valleys in Unit 2 are potentially artifacts of gas derived from below. The loss of water associated with the brief desiccation is likely to have initiated this discharge. This phenomenon came to an end after the later loading of marine water. Core data would be able to strengthen this interpretation but is at the moment unavailable. Hence, no deposition during MIS 3-2 is observed in this lake and lake level had to be below the depth of the Imrali ridge during this period.

Chirp sub-bottom profiles across the outer shelf of the western Black Sea reveal a succession of superimposed lacustrine deposits (Fig. 5) belonging to basinward prograding lowstand deltas (Aksu et al. 2002, Dimitrov 2010). On top of the youngest clinoforms are sand dunes and a berm like feature indicative of a paleoshoreface (Lericolais et al. 2009, Yanchilina 2016, Yanchilina et al. 2017). Where sampled, the youngest set of prograding strata are  $^{14}\text{C}$  dated to late MIS 3 through MIS 2 and contain lacustrine fauna (Yanchilina et al. 2017). The succession of parallel and prograding deposits indicates alternating highstands and lowstands. If one were to consider that these clinoforms were deposited in a near-shore subaqueous prodelta environment, they indicate the surface of the Black Sea-Lake was 80 to 90 mbsl during MIS 3.

## 5. Discussion

Geochemical and geophysical data suggest that Black Sea and Marmara Sea remained fresh and the hydrological budget was positive during most of MIS 3, with the exception of a period between 44 and 55 kyr B.P. The hydrologic budget must have remained positive in order for (1) the perched ponds not to have dried out and (2) to account for the similarity in the elevation of the surface of the Marmara and Black Sea-Lakes and their correspondence with elevations of the Dardanelles bedrock, to maintain outflow as suggested by geochemical data (i.e., identical  $\text{CaCO}_3$  during MIS 3 and 2, low  $\delta^{18}\text{O}$  of Sofular Cave stalagmites, and similar  $^{87}\text{Sr}/^{86}\text{Sr}$  during end of MIS 3/ 2).

The similarity between the present average elevation of the lake's surface and the elevation of the Dardanelles and Bosphorus Sills at ~65-80 mbsl confirms that the straits acted as outflow channels (i.e., a rivers) expelling Black and Marmara Sea-Lake freshwater to the



external ocean during MIS 3 and MIS 2. This also suggests that the Dardanelles bedrock sill was at or near (by a few meters) the relative sea level. It remains possible that RSL is below by a few meters the Dardanelle paleo-sill, if freshwater flux would have been able to sustain a certain pressure to deny any marine inflow (Dalziel 1991; Lane-Serff et al. 1997; Lambeck et al. 2007). The observation of a lower lake surface that indicates that the Bosphorus sill also must have been deeper than today, sitting at its bedrock at 80 mbsl. If the outlet sill was shallower, then the elevation of the foresets would likely have been higher. Substantial river entrenchment may have deepened its modern bedrock depth. For example, MIS 6, 8, 10, and 12 lowstand clinoforms in the region of Prince Islands (Supplementary Materials 2) are all at elevations as low or lower than the MIS 2 and 3 clinoforms. Thus the lake's ancient shorelines must have always had to have fallen to an elevation near to the modern bedrock elevation during each lacustrine period.

This set of independent geological archives provide RSL index with present elevation ranging between 70 and 90 mbsl. The present elevations of indexes are likely different than their paleo-elevations during MIS 3. The present elevations of indexes are likely different than their paleo-elevations during MIS 3. 10-20 m of regional subsidence has likely occurred since MIS 3, as the results of GIA associated with the overall ice-water budget in between the glacial MIS 3 time and today. This may place the RSL during MIS 3 at a maximum value of 80 m. During MIS 3, RSL was shallower than the ESL here, in response to the GIA associated with the transition from MIS 5 interglacial stage into MIS 3. This suggests that the ESL in the region was likely below 70 mbsl during the overall MIS 3 glacial stage. This threshold on ESL is in agreement with the results from U/Th dated coral terraces corrected for GIA (Yokoyama et al. 2001) that leads to coral-based global sea level reconstructions about ~58-111 mbsl (~45 to -110 mbsl if error is included) (Fig. 1e) (Yokoyama et al. 2001). Four of these coral-based ESL reconstructions during MIS 3 give a range of 58 to 70 mbsl and eight in the range of 70 to 80 mbsl. Our results on ESL supports the lower estimates obtained from scaling changes from the LR04 stack of benthic  $\delta^{18}\text{O}$  records (Bintanja et al. 2005), but does not entirely agree with changes in ESL from scaling changes from detrended planktonic  $\delta^{18}\text{O}$  records corrected for changes in temperature (Shakun et al. 2015). Our results differ from the ESL estimates from the U.S. Mid-Atlantic coast and the Yellow Sea deposits show the ocean surface was shallower than indicated by our observations during MIS 3. While these estimates serve as valuable surface of sea level information, they are currently limited by a lack of clear evidence of submersion by marine water and a reliance on dates from dune and channel sand. For the



Yellow Sea, since radiocarbon dates on shells from these sediments are at the limit of reliability, dating of the sand has been accomplished by OSL methods (Liu et al. 2010). The reflection profiles show that the sampled sand is from a channel fill within a dendritic drainage system, more likely of fluvial origin rather than sand from a marine transgression. Likewise, the suggested ESL peak of 40 mbsl during MIS 3 (Pico et al. 2017) in the Albermarle Embayment on the U.S. Mid-Atlantic coast is based on OSL-dated sands sampled from eolian dunes with interbedded paleo-sol and resting on peat (Mallison et al. 2008). The diagnostic evidence of a marine transgression is from mollusk shells under the peat and attributed to MIS 5. Close inspection of analyses from both the Yellow Sea and U.S. Mid-Atlantic coast suggests assigning a marine transgression to these two areas needs further scrutiny and cannot be concretely assigned to a eustatic sea level highstand during MIS 3.

## 6. Conclusions

Paleosalinity interpretations from measurements of Ca and  $\text{CaCO}_3$ , porewater  $\text{Cl}^-$ ,  $\delta^{18}\text{O}$  and  $^{87}\text{Sr}/^{86}\text{Sr}$  composition of mollusks from Black Sea and Marmara Seas,  $\delta^{18}\text{O}$  composition of the Sofular Cave stalagmite records indicate the two seas were freshwater lakes, connected, and outflowing to the Mediterranean Sea for the majority of MIS 3, with the possible exception of a period encompassing 55 to 44 kyr B.P. Lack of marine entry through most of this period is supported by evidence of ponded/perched lakes in the Marmara Sea that lack any observable marine deposits. In the future, it is critical to obtain  $\delta^{18}\text{O}$  and  $^{87}\text{Sr}/^{86}\text{Sr}$  measurements in carbonates for the Black and Marmara Sea-Lakes during this period to make more robust conclusions about the paleo-connectivity and outflow of these basins. Low  $\delta^{18}\text{O}$  of  $\sim -6\text{‰}$  and  $^{87}\text{Sr}/^{86}\text{Sr}$  of  $\sim 0.7088$  would show that the water in these lakes was fresh and fed by Black Sea river water.

Clinofolds, wave cut cliffs and corresponding terraces indicate that the lake level of the two sea-lakes was at 80 to 90 mbsl during this period, suggesting a positive water budget and outflow. Both of the sills, the Bosphorus that connects the Black Sea with the Marmara Sea and the Dardanelles that connects the Marmara Sea with the Mediterranean Sea were at the level of the paleoshoreline. If the RSL on the Mediterranean side of the Dardanelles sill was higher than the level of the sill, there should be indication of marine entry. As there is not, we conclude, with taking wave base into consideration, the RSL must have been at or below the level of the sills, maximum at 65-70 mbsl, for the majority of the period with the exception of 55 to 44 kyr B.P. ESL should have been even lower during this period, as 10-20 m of local



376 subsidence would have occurred as a consequence of the changes in the distribution of ice  
377 sheets in Eurasia from MIS 3 to present.

378

## 379 References

380

- 381 Aksu, A. E., R. N. Hiscott, M. A. Kaminski, P. J. Mudie, H. Gillespie, T. Abrajano and D.  
382 Yaşar: Last glacial-Holocene paleoceanography of the Black Sea and Marmara Sea:  
383 stable isotopic, foraminiferal and coccolith evidence, *Marine Geology*, 190, 119-49,  
384 10.1016/S0025-3227(02)00345-6, 2002.
- 385 Aksu, A. E., C. Yaltirak and R. N. Hiscott: Quaternary paleoclimatic -paleoceanographic and  
386 tectonic evolution of the Marmara Sea and environs, *Marine Geology*, 190, 9-18,  
387 2002.
- 388 Aloisi, G., G. Soulet, P. Henry, K. Wallmann, R. Sauvestre, C. Vallet-Coulomb, C. Lécuyer  
389 and E. Bard: Freshening of the Marmara Sea prior to its post-glacial reconnection to  
390 the Mediterranean Sea, *Earth and Planetary Science Letters*, 413, 176-85,  
391 10.1016/j.epsl.2014.12.052, 2015.
- 392 Badertscher, S., D. Fleitmann, H. Cheng, R. L. Edwards, O. M. Göktürk, A. Zumbühl, M.  
393 Leuenberger and O. Tüysüz: Pleistocene water intrusions from the Mediterranean and  
394 Caspian seas into the Black Sea, *Nature Geoscience*, 4, 236-39, 10.1038/NGEO1106,  
395 2011.
- 396 Bailey, T. R., J. M. McArthur, H. Prince and M. F. Thirwall: Dissolution methods for  
397 strontium isotope stratigraphy: Whole rock analysis, *Chemical Geology*, 167, 313-19,  
398 2000.
- 399 Bintanja, R., R. S. W. van De Wal and O. Johannes: Modelled atmospheric temperatures and  
400 global sea levels over the past million years, *Nature*, 437, 125-28, 2005.
- 401 Birck, J.-L.: Precision K-Rb-Sr isotopic analysis; applications to Rb-Sr chronology, *Chemical*  
402 *Geology*, 56, 73-83, 1986.
- 403 Çagatay, M. N., Water Exchange Between Mediterranean and Black Seas During Late  
404 Glacial-Holocene: Evidence from Marmara and Black Seas, Annual Meeting  
405 Geological Society of America, Seattle. WA, Geological Society of America, 2003.
- 406 Çagatay, M. N., K. Eriş, W. B. F. Ryan, Ü. Sancar, A. Polonia, S. Akçer, D. Biltekin, L.  
407 Gasperini, N. Görür, G. Lericolais and E. Bard: Late Pleistocene-Holocene evolution  
408 of the northern shelf of the Sea of Marmara, *Marine Geology*, 265, 87-100,  
409 10.1016/j.margeo.2009.06.011, 2009.
- 410 Çagatay, M. N., S. Wulf, Ü. Sancar, A. Özmaral, L. Vidal, P. Henry, O. Appelt and L.  
411 Gasperini: The tephra record from the Sea of Marmara for the last ca. 70 ka and its  
412 paleoceanographic implications, *Marine Geology*, 361, 96-100,  
413 10.1016/j.margeo.2015.01.005, 2015.
- 414 Cutler, K. B., R. L. Edwards, F. W. Taylor, H. Cheng, J. Adkins, C. D. Gallup, P. M. Cutler,  
415 G. S. Burr and A. L. Bloom: Rapid sea-level fall and deep-ocean temperature change  
416 since the last interglacial period, *Earth and Planetary Science Letters*, 206, 253-71,  
417 10.1016/S0012-821X(02)01107-X, 2003.
- 418 Dansgaard, W., S. J. Johnsen, H. B. Clausen, D. Dahl-Jensen, N. Gundenstrup, C. U.  
419 Hammer, C. S. Hvidberg, J. P. Steffensen, A. E. Sveinbjörnsdóttir, J. Jouzel and G.  
420 Bond: Evidence for general instability of past climate from a 250-kyr ice core, *Nature*,  
421 364, 218-20, 1993.
- 422 Deuser, W. G.: Late-Pleistocene and Holocene history of the Black Sea as indicated by stable  
423 isotope studies, *Jour. Geophys. Res.*, 77, 1071-77, 1972.



- 424 Dimitrov, D., Geology and non-traditional resources of the Black Sea, Germany, Lambert  
425 Akademik Publishing AG, 2010.
- 426 Ergin, M., E. Uluadam, K. Sarikavak, Ş. Keskin, E. Gökaşan and H. Tur, Late Quaternary  
427 sedimentation and tectonics in the submarine Sarkoy Canyon, western Marmara Sea  
428 (Turkey). The Geodynamics of the Aegean and Anatolia, T. Taymaz, Y. Yilmaz and  
429 Y. Dilek, London, Special Publications, 291, 231-57, 2007.
- 430 Fleitmann, D., H. Cheng, S. Badertscher, R. L. Edwards, M. Mudelsee, O. M. Göktürk, A.  
431 Fankhauser, R. Pickering, C. C. Raible, A. Matter, J. Kramers and O. Tüysüz: Timing  
432 and climatic impact of Greenland interstadials recorded in stalagmites from northern  
433 Turkey, Geophysical Research Letters, 36, 10.1029/2009GL040050, 2009.
- 434 Genov, I.: Seismostratigraphy and the last Black Sea level changes, Geologie, 68, 1419-24,  
435 2015.
- 436 Gokasan, E., M. Ergin, M. Ozyalvac, I. H. Sur, H. Tur, T. Gorum, T. Ustaomer, F. G. Batuk,  
437 H. Alp, H. Birkan, A. Turker, E. Gezgin and M. Ozturan: Factors controlling the  
438 morphological evolution of the Canakkale Strait (Dardanelles, Turkey), Geo-Mar  
439 Letters, 28, 107-29, 2008.
- 440 Gökaşan, E., T. Hüseyin, M. Ergin, T. Görüm, F. G. Batuk, N. Sağci, T. Ustaömer, O. Emem  
441 and H. Alp: Late Quaternary evolution of the Çanakkale Strait region (Dardanelles,  
442 NW Turkey): implications of a major erosional event for the postglacial  
443 Mediterranean-Marmara Sea connection, Geo-Mar Letters, 30, 113-31,  
444 10.1007/s00367-009-0166-2, 2010.
- 445 Grall, C., P. Henry, Y. Thomas, G. K. Westbrook, M. N. Çağatay, B. Marsset, H. Saritas, G.  
446 Çifçi and L. Géli: Slip rate estimation along the western segment of the Main  
447 Marmara Fault over the last 405-490 ka by correlating mass transport deposits,  
448 Tectonics, 32, pp. 1587-601, 2013.
- 449 Henderson, G. M., D. J. Martel, R. K. O'Nions and N. J. Shackleton: Evolution of seawater  
450 Sr-87/Sr-86 over the last 400-ka - the absence of glacial interglacial cycles, Earth and  
451 Planetary Science Letters, 128, 1994.
- 452 Hiscott, R. N., A. E. Aksu, D. Yasar, M. A. Kaminski, P. J. Mudie, V. Kostylev, J. C.  
453 MacDonald and A. R. Lord: Deltas south of the Bosphorus record persistent Black Sea  
454 outflow to the Marmara Sea since ~10 ka, Marine Geology, 190, 95-118, 2002.
- 455 Karakilcik, H., U. Can Unlugenc and M. Okyar: Late glacial-Holocene shelf evolution of the  
456 Sea of Marmara west of Istanbul, Journal of African Sciences, 100, 365-78,  
457 10.1016/j.jafrearsci.2014.06.003, 2014.
- 458 Lambeck, K., Y. Yokoyama and T. Purcell: Into and out of the Last Glacial Maximum: sea-  
459 level change during Oxygen Isotope Stages 3 and 2, Quaternary Science Reviews, 21,  
460 343-60, 2002b.
- 461 Lericolais, G., C. Bulois, H. Gillet and F. Guichard: High frequency sea level fluctuations  
462 recorded in the Black Sea since the LGM, Global Planet Change, 66, 65-75,  
463 10.1016/j.gloplacha.2008.03.010, 2009.
- 464 Liu, Z. and K.-F. Huang: Clay mineral distribution in surface sediments of the northeastern  
465 South China Sea and surrounding fluvial discharge basins: Source and transport,  
466 Marine Geology, 277, 48-60, 2010.
- 467 Major, C., S. Goldstein, W. Ryan, G. Lericolais, A. M. Piotrowski and I. Hajdas: The co-  
468 evolution of Black Sea level and composition through the last deglaciation and its  
469 paleoclimatic significance, Quatern. Sci. Rev., 25, 2031-47,  
470 doi:10.1016/j.quascirev.2006.01.032, 2006.
- 471 Mallison, D. and G. Brook: Optically stimulated luminescence age controls on late  
472 Pleistocene and Holocene coastal lithosomes, North Carolina, USA, Quaternary  
473 Research, 69, 97-109, 2008.



- 474 McHugh, C. M. G., D. Gurung, L. Giosan, W. B. F. Ryan, Y. Mart, U. Sancar, L. Burckle  
475 and M. N. Çağatay: The last reconnection of the Marmara Sea (Turkey) to the World  
476 Ocean: A paleoceanographic and paleoclimatic perspective, *Marine Geology*, 255,  
477 64-82, 10.1016/j.margeo.2008.07.005, 2008.
- 478 Members, E. C.: One-to-one coupling of glacial climate variability in Greenland and  
479 Antarctica, *Nature*, 444, 195, 2006.
- 480 Nowaczyk, N. R., H. W. Arz, U. Frank, J. Kind and B. Plessen: Dynamics of the Laschamp  
481 geomagnetic excursion from Black Sea sediments, *Earth and Planetary Science*  
482 *Letters*, 351-352, 54-69, 10.1016/j.epsl.2012.06.050, 2012.
- 483 Palmer, M. R. and J. M. Edmond: The strontium budget of the modern ocean, *Earth and*  
484 *Planetary Science Letters*, 92, 11-26, 1989.
- 485 Peltier, W. R. and R. G. Fairbanks: Global glacial ice volume and Last Glacial Maximum  
486 duration from an extended Barbados sea level record, *Quaternary Science Reviews*,  
487 25, 3322-37, 10.1016/j.quascirev.2006.04.010, 2006.
- 488 Pico, T., J. R. Creveling and J. X. Mitrovica: Sea-level records from the U.S. mid-Atlantic  
489 constrain Laurentide Ice Sheet extent during Marine Isotope Stage 3, *Nature*  
490 *Communications*, 10.1038/ncomms15612, 2017.
- 491 Pico, T., J. X. Mitrovica, K. L. Ferrier and J. Braun: Global ice volume during MIS 3 inferred  
492 from a sea-level analysis of sedimentary core records in the Yellow River Delta,  
493 *Quaternary Science Reviews*, 152, 72-79, 2016.
- 494 Rochon, A., P. J. Mudie, A. E. Aksu and H. Gillespie: *Ptericysta* Gen. Nov.: A new  
495 dinoflagellate cyst from pleistocene glacial-stage sediments of the Black and  
496 Marmara Seas, *Palynology*, 26, 95-105, 2002.
- 497 Shakun, J. D., D. W. Lea, L. E. Lisiecki and M. E. Raymo: An 800-kyr record of global  
498 surface ocean  $\delta^{18}\text{O}$  and implications for ice volume-temperature coupling, *Earth and*  
499 *Planetary Science Letters*, 426, 58-68, 2015.
- 500 Siddall, M., E. J. Rohling, W. G. Thompson and C. Waelbroeck: Marine isotope stage 3 sea  
501 level fluctuations: data synthesis and new outlook, *Review of Geophysics*, 46,  
502 10.1029/2007RG000226, 2008.
- 503 Smith, A. D., T. Taymaz, F. Oktay, H. Yuce, B. Alpar, H. Basaran, J. A. Jackson, S. Kara  
504 and M. Simsek: High resolution seismic reflection profiling in the sea of Marmara  
505 (northwest Turkey): Late Quaternary sedimentation and sea-level changes, *Bulletin of*  
506 *Geologicak Society of America*, 107, 923-36, 10.1130/0016-7606(1995), 1995.
- 507 Soulet, G., G. Delaygue, C. Vallet-Coulomb, M. E. Böttcher, C. Sonzogni, G. Lericolais and  
508 E. Bard: Glacial hydrologic conditions in the Black Sea reconstructed using  
509 geochemical pore water profiles, *Earth and Planetary Science Letters*, 296, 57-66,  
510 10.1016/j.epsl.2010.04.045, 2010.
- 511 Van Daele, M., A. van Welden, J. Moernaut, C. Beck, F. Audermard, J. Sanchez, F. Jouanne,  
512 E. Carrillo, G. Malavé, A. Lemus and M. De Batist: Reconstruction of Late-  
513 Quaternary sea- and lake-level changes in a tectonically active marginal basin using  
514 seismic stratigraphy: The Gulf of Cariaco, NE Venezuela, *Marine Geology*, 279, 37-  
515 51, 2011.
- 516 Vardar, D., K. Öztürk, C. Yaltirak, B. Alpar and H. Tur: Late Pleistocene-Holocene evolution  
517 of the southern Marmara shelf and sub-basins: middle strand of the North Anatolian  
518 fault, southern Marmara Sea, Turkey, *Marine Geophysical Research*, 35, 69-85, 2014.
- 519 Vidal, L., G. Ménot, C. Joly, H. Bruneton, F. Rostek, M. N. Çağatay, C. Major and E. Bard:  
520 Hydrology in the Sea of Marmara during the last 23 ka: Implications for timing of  
521 Black Sea connections and sapropel deposition, *Paleoceanography*, 25,  
522 10.1029/2009PA001735, 2010.





15

- 523 Yaltirak, C., M. Sakinc, A. E. Aksu, R. N. Hiscott, B. Galleb and U. B. Ulgen: Late  
 524 Pleistocene uplift history along the southwestern Marmara Sea determined from  
 525 raised coastal deposits and global sea-level variations, *Marine Geology*, 192, 283-305,  
 526 10.1016/S0025-3227(02)00351-1, 2002.
- 527 Yanchilina, A. G. (2016). Excess freshwater outflow from the Black Sea-Lake during glacial  
 528 and deglacial periods and delayed entry of marine water in the early Holocene require  
 529 evolving sills, Columbia University.
- 530 Yanchilina, A. G., W. B. F. Ryan, J. F. McManus, P. Dimitrov, D. Dimitrov, K. Slavova and  
 531 M. Filipova-Marinova: Compilation of geophysical, geochronological, and  
 532 geochemical evidence indicates a rapid Mediterranean-derived submergence of the  
 533 Black Sea's shelf and subsequent substantial salinification in the early Holocene,  
 534 *Marine Geology*, 383, 14-34, 10.1016/j.margo.2016.11.001, 2017.
- 535 Yokoyama, Y., P. De Deckker, K. Lambeck, P. Johnston and K. Fifield: Sea-level at the Last  
 536 Glacial Maximum: evidence from northwestern Australia to constrain ice volumes for  
 537 oxygen isotope stage 2, *Paleoceanography, Palaeoclimatology, Palaeoecology*, 165,  
 538 281-97, 10.1016/S0031-0182(00)00164-4, 2001.

## 539 Acknowledgments

540 The authors would like to acknowledge the crew of the Akademik 2009 and 2011  
 541 expeditions, Louise Bolge and Leo Pena for assistance with the geochemical analyses,  
 542 Giovanni Aloisi, Helge Arz, Namik Çağatay, Samuel Goldberg for generating GIA corrections  
 543 and helpful discussion, Candace Major for the  $^{87}\text{Sr}/^{86}\text{Sr}$  records from the Sea of Marmara,  
 544 Guillaume Soulet, and Bill Thompson for sharing datasets employed to reach our conclusions.

## 547 Figures

548 Figure 1:

550





16

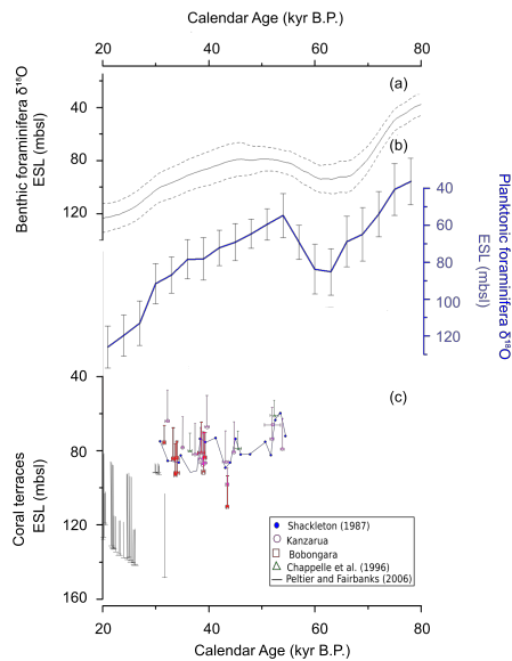


**Figure 1.** Prior sea-level reconstructions for MIS 3. **(a)** ESL reconstruction using inverse climate ice-sheet modelling from  $\delta^{18}\text{O}$  LR04 record (Bintanja et al. 2005). **(b)** ESL derived from extraction of ice volume from planktonic  $\delta^{18}\text{O}$  (Shakun et al. 2015). **(c)** ESL reconstruction corrected for regional uplift and GIA (Yokoyama et al. 2001, Peltier et al. 2006).

Figure 2:

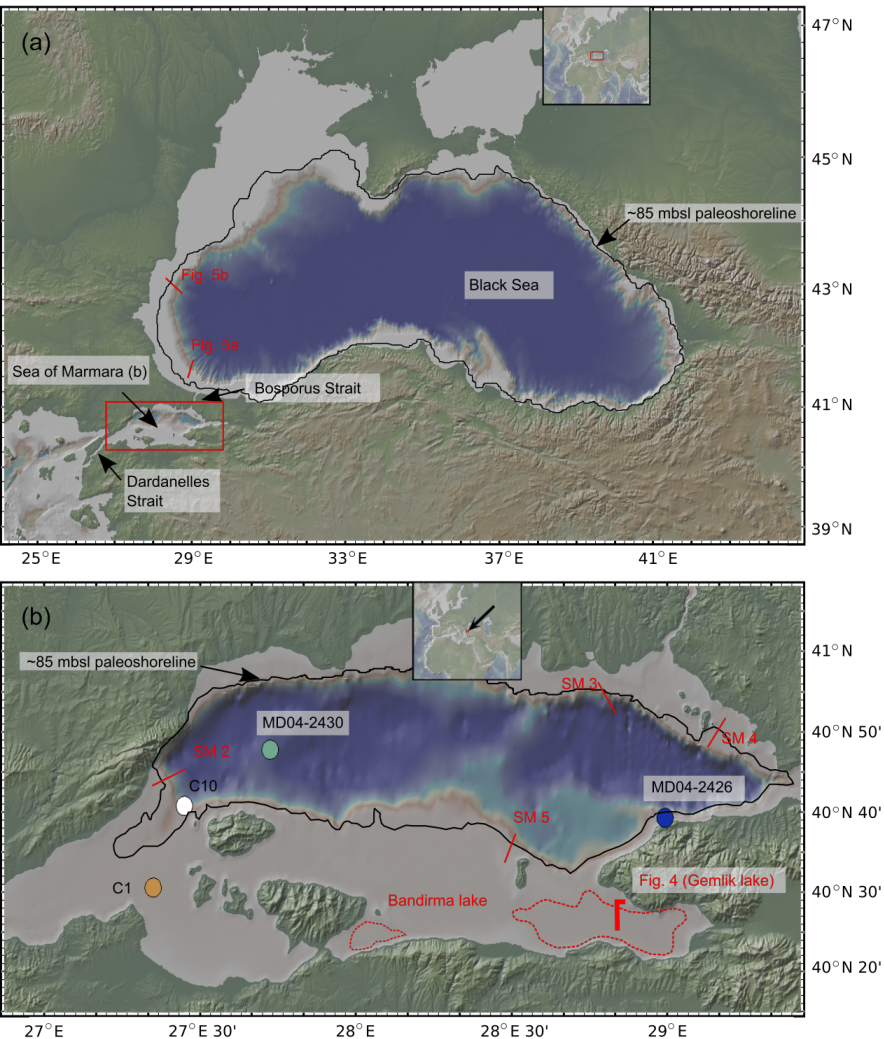


**Figure 2:** Map of the Black Sea (a) and Sea of Marmara (b). Important geographical features are indicated. (a) Location of the Black Sea, Sea of Marmara relative to the Black Sea, Bosphorus Strait and the Dardanelles Strait. Also are indicated the seismic profiles provided in figure 5a and 5b. The location of the ~85 mbsl paleoshoreline is pointed out. (b) Indicated are the locations of the Gemlik and Bandirma perched lakes in addition to the location of the seismic profile for Gemlik lake presented in Fig. 4. Also are indicated the locations of the cores MD04-2426, MD04-2430, C1, and C10. The locations of the seismic profiles provided in the supplementary materials are also indicated as SM 2, SM 3, SM 4, and SM5.

Figure 3:



18

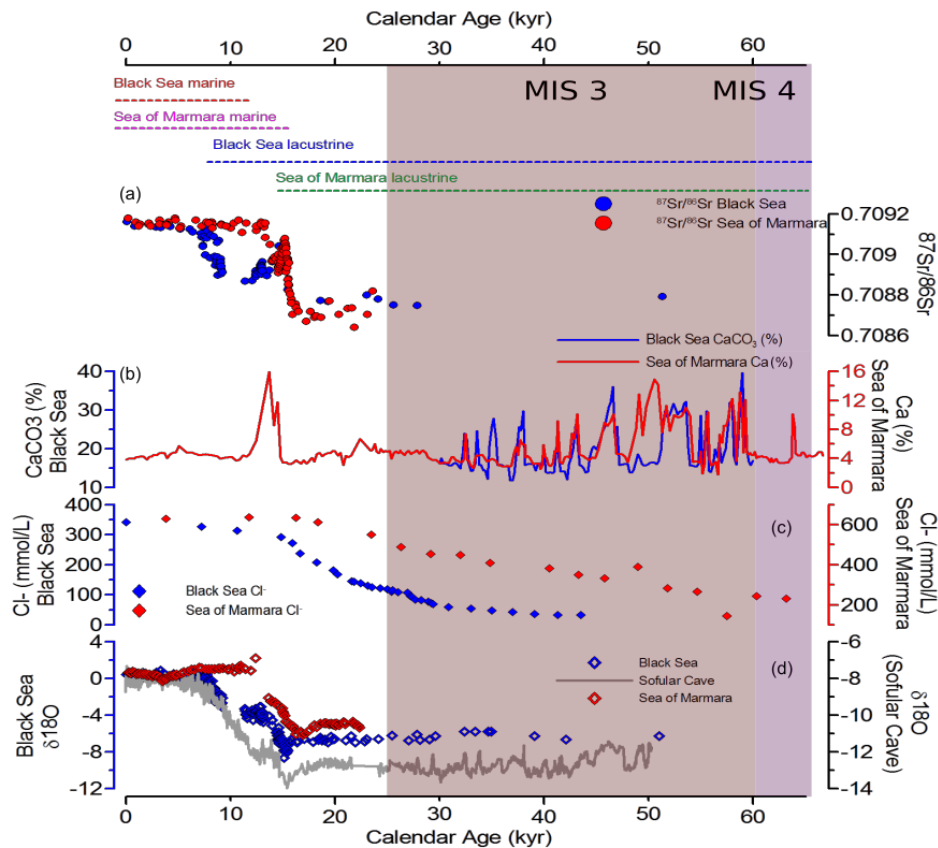
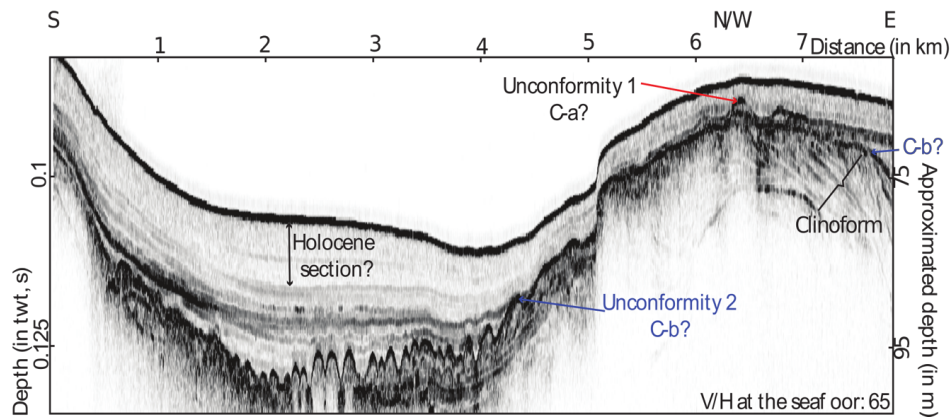


**Figure 3.** Changes in geochemical proxies during MIS 3. (a)  $^{87}\text{Sr}/^{86}\text{Sr}$  from the Black and Marmara Sea-Lakes (C.O. Major, National Science Foundation)  $^{87}\text{Sr}/^{86}\text{Sr}$  from the Black Sea is taken from the work of Major et al. (2006), Yanchilina et al. (2017), Yanchilina et al. (2019); the  $^{87}\text{Sr}/^{86}\text{Sr}$  from the Marmara Sea is what is what measured in the present manuscript. (b)  $\text{CaCO}_3$  from the Black Sea-Lake (Nowaczyk et al. 2012) and Ca from the Marmara Sea-Lake (Çağatay et al. 2015). (c) Black Sea and Sea of Marmara porewater chlorinity, respectively (Soulet et al. 2010, Aloisi et al. 2015). (d)  $\delta^{18}\text{O}$  from the Black Sea (blue), the Sea of Marmara (red) (Vidal et al. 2010) and Sofular Cave (grey)  $\delta^{18}\text{O}$  (Badertscher et al. 2011).



19

600 Figure 4:  
601



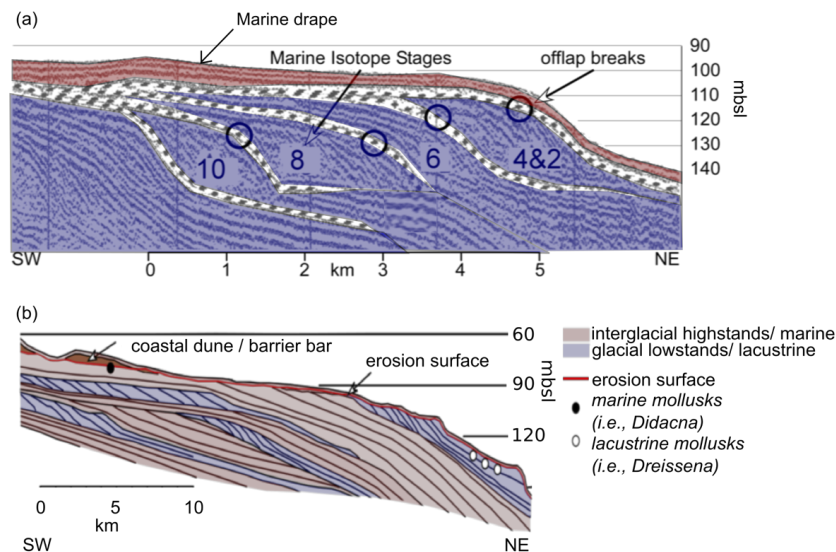
602  
603  
604  
605  
606 **Figure 4.** Chirp sub-bottom profile across the Gemlik Bay. 2 unconformities on the shore of  
607 the Bay, only one in the lake. The shallowest one has been estimated to be associated with the  
608 Last Marine-Lacustrine transition and the deepest.

609  
610  
611  
612  
613  
614  
615  
616  
617  
618  
619  
620  
621  
622  
623  
624  
625  
626  
627  
628  
629  
630  
631  
632  
633  
634  
635



20

636 Figure 5:  
637



638  
639  
640  
641  
642  
643  
644  
645  
646  
647  
648  
649  
650  
651

**Figure 5.** Reflection profiles on the SW shelf of the Black Sea. **(a)** Succession of superimposed prograding clinoforms adopted from a previously published illustration (Fig. 11c) (Aksu et al. 2002) with offlap breaks indicating present and past locations of lowstand deltas at the shelf edge. Numbers are inferred MIS stages when the Black Sea was a freshwater lake. **(b)** A similar succession with thinner glacial-age lowstand clinoforms (blue) and thicker interglacial highstand deposits adopted from an earlier published XIX profile retrieved from R/V Hydrograph in 1998 (Genov 2015). White circles indicate sampling of lacustrine mollusks of MIS 2 and 3 age; black circles indicate sampling of marine mollusks presumable of MIS 5 age (Dimitrov 2010). Coastal dunes place the MIS 3 and 2 shorelines at elevations between 80 and 90 mbsl.